AD-A141 379 SUPERSONIC MOLECULAR JET STUDIES OF TOLUENE-HELIUM AND TOLUENE-METHANE CL..(U) COLORADO STATE UNIV FORT COLLINS DEPT OF CHEMISTRY M SCHAUER ET AL. 15 MAY 84 TR-13 N00014-79-C-0647 1/1

UNCLASSIFIED F/G 7/4 NL

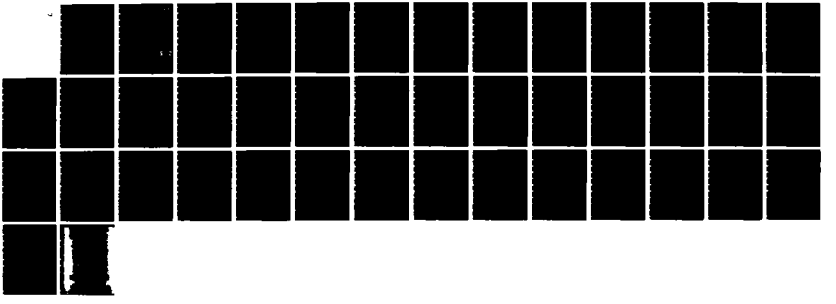

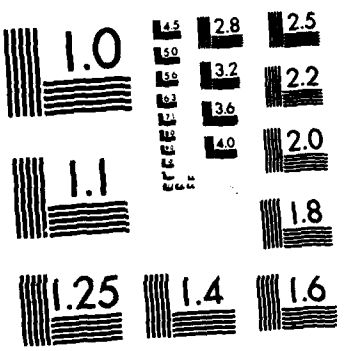

12

OFFICE OF NAVAL RESEARCH
Contract N00014-79-C-0647
TECHNICAL REPORT #13

SUPERSONIC MOLECULAR JET STUDIES OF TOLUENE-HELIUM AND TOLUENE-METHANE CLUSTERS

by

Mark Schauer, K. Law, and E.R. Bernstein

Prepared for Publication
in the
Journal of Chemical Physics

Department of Chemistry
Colorado State University
Fort Collins, Colorado 80523

May 15, 1984

SECURITY CLASSIFICATION OF THIS PAGE *(When Data Entered)*

REPORT DOCUMENTATION PAGE		READ INSTRUCTIONS BEFORE COMPLETING FORM
1. REPORT NUMBER Technical report #13	2. GOVT ACCESSION NO.	3. RECIPIENT'S CATALOG NUMBER
4. TITLE *(and Subtitle)* Supersonic Molecular Jet Studies of Toluene-Helium and Toluene-Methane Clusters		5. TYPE OF REPORT & PERIOD COVERED Technical Report 6. PERFORMING ORG. REPORT NUMBER
7. AUTHOR(s) Mark Schauer, K. Law and E.R. Bernstein		8. CONTRACT OR GRANT NUMBER(s) N00014-79-C-0647
9. PERFORMING ORGANIZATION NAME AND ADDRESS Colorado State University Department of Chemistry Fort Collins, Colorado 80523		10. PROGRAM ELEMENT, PROJECT, TASK AREA & WORK UNIT NUMBERS
11. CONTROLLING OFFICE NAME AND ADDRESS Office of Naval Research Arlington, Virginia 22217		12. REPORT DATE May 15, 1984 13. NUMBER OF PAGES 26
14. MONITORING AGENCY NAME & ADDRESS*(if different from Controlling Office)*		15. SECURITY CLASS. *(of this report)* Unclassified 15a. DECLASSIFICATION/DOWNGRADING SCHEDULE

16. DISTRIBUTION STATEMENT *(of this Report)*

DISTRIBUTION STATEMENT A
Approved for public release;
Distribution Unlimited

17. DISTRIBUTION STATEMENT *(of the abstract entered in Block 20, if different from Report)*

18. SUPPLEMENTARY NOTES

19. KEY WORDS *(Continue on reverse side if necessary and identify by block number)*

time of flight mass spectroscopy, two photon ionization, supersonic molecular jet, intramolecular vibrational distribution, van der Waals clusters, dispersed emission, fluorescence excitation, Toluene, Toluene-Helium and Toluene-Methane solvation.

20. ABSTRACT *(Continue on reverse side if necessary and identify by block number)*

The techniques of fluorescence excitation (FE), dispersed emission (DE), and 1- and 2-color time of flight mass spectroscopy (TOFMS) have been employed to study van der Waals clusters of toluene-helium (TolHe) and toulene-methane ($TolCH_4$) formed in a supersonic molecular jet. Spectral shifts for the toluene $^1B_2 \leftarrow {}^1A_1$ transition have been characterized for $TolHe_{1,2}$ and $Tol(CH_4)_{1,2}$. The van der Waals stretching frequencies (ν_1) in the excited states of these clusters have been identified. The ground

DD FORM 1 JAN 73 1473 EDITION OF 1 NOV 65 IS OBSOLETE

Unclassified

SECURITY CLASSIFICATION OF THIS PAGE *(When Data Entered)*

state stretch (V_1) for TolHe has also been found; it is quite similar to the TolHe V_1. The binding energies (D_o) for Tol-He clusters lie between 75 and 90cm^{-1} and those for Tol-CH_4 clusters lie between 533 and 739cm^{-1}. The coordination of a third solvent molecule to those clusters generates a broad spectrum whose shift is close to the limiting value for a large (X>3) cluster. A comparison between these data and methane solution data is presented.

I. INTRODUCTION

A number of recent supersonic molecular jet studies have dealt with the generation and characterization of van der Waals (vdW) molecules formed between a solute species (tetrazine[1], aniline[2], benzene[3], etc.) and small solvent molecules (helium, argon, methane, etc.). Several reports have discussed vdW clusters as model solute/solvent cage systems.[2,4] Previous work from our laboratory[2a,b] has related the observed spectroscopic properties of vdW clusters with spectroscopic properties of cryogenic liquid solutions.[5] The comparison between gas phase clusters and simple solutions has proved useful: it has shed some light on both solute/solvent cage structure and dynamics. Various cluster processes, such as vibrational predissociation (VP) and intramolecular vibrational redistribution (IVR), can be invoked to rationalize the behavior of a solute molecule in solution. Specifically, it has been possible to relate aniline (An) methane cluster data to aniline cryogenic solution behavior.[2b]

Toluene (Tol) is perhaps a better solute molecule than An with which to pursue this comparison: liquid state data have already been published from this laboratory[5a] dealing with Tol dissolved in several small cryogenic hydrocarbon solvents. Fluorescence excitation (FE) and dispersed emission (DE) spectra of Tol in a molecular jet have already been reported.[6] In addition, the data presented in this paper for Tol should complement that obtained for An, since An and Tol have similar geometries, molecular properties, and interactions with small hydrocarbons.

Two problems arise in the study of Tol vdW clusters in a molecular jet: several low frequency Tol vibrational features have not previously been assigned, and the Tol dimer [Tol_2] FE spectrum overlaps with and obscures some of the cluster transitions. Assignments for weak features in the Tol

spectrum have to be made in order to understand the major features in the cluster DE spectra. Two-color time of flight mass spectroscopy (2-color TOFMS) studies allow separation of monomer, cluster, and Tol dimer features quite clearly, as will be shown below.

This paper will present data on Tol-He and Tol-CH_4 vdW clusters: the elaborate $(Tol)_x$ (x = 2,3,4...) spectra will be treated in a separate publication. The results of our investigations on these two cluster systems will be compared with our previous data for An-He and An-CH_4 vdW clusters[2a,b] and for Tol dissolved in cryogenic liquid solutions.[5a] The Results Section examines FE, DE, and 1- and 2-color TOFMS spectra for the Tol-He and the Tol-CH_4 systems. The Discussion Section will focus on the physical properties of the vdW clusters and their dynamical processes. Properties of the Tol-CH_4 clusters will be compared with those of aniline-methane clusters and toluene-methane liquid solutions.

II. EXPERIMENTAL PROCEDURES

The supersonic molecular jet apparatus currently employed in this work has been described previously[2a,b]: laser power and beam conditions are the same as given in these references. All spectra are obtained with low enough power to avoid saturation in both pump and ionization processes. Three different studies are carried out for this work. Fluorescence excitation (FE) experiments monitor the total fluorescence of all species in the beam as the laser wavelength is scanned through the solute absorption region. For a solute species with high quantum yield, the total emission is directly related to absorption. The spectrum thus obtained is proportional to a composite absorption spectrum of all species in the molecular jet. Dispersed emission (DE) spectra are obtained as a particular feature in the FE spectrum is excited and the ensuing emission is resolved with a single grating scanning monochromator. DE spectra can consist of emission features from more than one species in the beam due to overlap of absorption peaks. Laser intensity for both FE and DE experiments is kept well below 2 mj/pulse to avoid saturation. The most selective experiment for species identification is time of flight mass spectroscopy (TOFMS). Ionization is accomplished selectively by either 1- or 2-color resonance enhanced 2 photon ionization. Two detection modes for the TOFMS can be employed: the intensity in a specific mass channel can be monitored as the pump beam is tuned; or, the time base of the TOFMS can be swept to detect all ion masses arriving at the detector for the duration of the experiments. One-color TOFMS is typically more intense than 2-color TOFMS; however, the 2-color excitation does not cause ion fragmentation and, thereby,loss of mass selectivity. In the 2-color TOFMS experiment the pump beam is always maintained at a low intensity (~100 μj/pulse) in order to insure that 1-color TOFMS does not occur. Blocking the ionization beam in the

2-color TOFMS experiment results in no appreciable TOFMS signal. Scanning the wavelength of the pump beam in a 2-color TOFMS experiment and detecting at a particular mass channel results in an absorption spectrum of the particular mass species monitored.

Both CW (25 μm orifice) and pulse (500 μm orifice) nozzles are used with the TOFMS experiments. The pulsed nozzle is advantageous in these experiments because of its large nozzle diameter and low duty cycle. The relative distance between the nozzle and the ionization region of the TOFMS is reduced from 21,320 nozzle diameters for the CW nozzle to 1066 for the pulsed nozzle; this reduction should lead to a factor of 400 increase in beam density, and thereby signal intensity, at the TOFMS. In practice the signal increase in the Tol mass channel is about a factor of 50 for the pulsed nozzle with respect to the CW nozzle.

Toluene is treated in the same manner as previously described for aniline[2a,b]. Aldrich spectroscopic grade toluene is used without purification. The carrier gas, either pure helium or a mixture of helium and methane, is passed over liquid toluene in a stainless steel trap at room temperature. The nozzle is also maintained at ambient temperature. The concentration of toluene in the beam varies as a function of the backing pressure (P_o).

III. RESULTS

In order to interpret the toluene van der Waals cluster data, it is quite useful to assign the toluene features in the regions encompassing the Tol 0_0^0 and Tol $6a_0^1$. The tentative assignments suggested here are based on toluene previously published[7] IR spectra and on the aniline electronic spectrum. The lowest frequency peaks observable above the Tol 0_0^0 (Fig. 1 and Table I) have been previously identified as hot bands of the methyl torsion modes.[6a] Molecular jet spectra, however, demonstrate that the features at 53 and 76 cm^{-1} are not hot bands, as their intensity relative to the Tol 0_0^0 intensity does not vary over a wide range of backing pressures (50 to 800 psi). These features are labeled T_o^x and T_o^y (x and y denote unknown quanta of this methyl torsional motion in the excited state). The two peaks at 288 and 291 cm^{-1} above the Tol 0_0^0 are assigned as $10b_0^2$ and $16a_0^2$, primarily due to the similarity of these peaks to analogous features in the aniline spectrum. Based on toluene IR data, the bands at 329 cm^{-1} and 368 cm^{-1} may be 15_0^1 and $16b_0^1$, respectively. The doubling of the $6a_0^1$ peak in the absorption spectrum of toluene has been attributed to Fermi resonance between $6a^1$ and an unidentified level.

These two regions of the toluene spectrum also contain features that are not associated with free molecular toluene. The peak at -19.7 cm^{-1} relative to the Tol 0_0^0 and a similar peak near $6a_0^1$ are due to absorption of the $(Tol)_2$ species. Preliminary 2-color TOFMS of the Tol dimer reveals a complicated broad structure with a sharp peak at -19.7 cm^{-1} from the Tol 0_0^0 and intensity on both the high and low energy sides of the Tol 0_0^0. The dimer spectra will be studied more extensively in the near future.

Tol-He

The FE spectra of various vibronic bands of the Tol-He system clearly show $TolHe_x$ vdW peaks to the high energy side of the Tol peaks. The 0_0^0 region (Fig. 2) and the $6b_0^1$ region (Fig. 3) evidence similar patterns. TolHe and $TolHe_2$ vibronic features exhibit a small additive blue shift with respect to comparable Tol vibronic transitions: peaks due to Tol-He vdW vibrational additions to these cluster vibronic origins are found further to the blue. The $6a_0^1$ region (Fig. 4) looks qualitatively similar to the 0_0^0 and $6b_0^1$ regions; however, congestion due to the apparent Fermi resonance of $6a^1$ makes assignments difficult.

The 2-color TOFMS data for various species in the 0_0^0 region in general confirm the above qualitative identification and generate species specific assignments. Fig. 5 presents the 2-color TOFMS for Tol, TolHe, and $TolHe_2$: a small additive successive shift to higher energy is evident between these three origins. In addition, the vdW stretching vibrational mode progression can be uniquely identified (Figs. 5 and 6) for each species. The $TolHe_3$ spectrum is, however, broad and somewhat structured with a non-additive blue shift.

An expanded trace of the TolHe and $TolHe_2$ 2-color TOFMS, Fig. 6, shows the vdW stretching modes in more detail (see also Table II). The stretching frequency in both species is nearly the same. The stretching progression can be employed to estimate the dissociation energy D_o by fitting the frequencies to a Morse potential oscillator in the usual fashion: an estimate of $D_o \sim 30\ cm^{-1}$ for TolHe obtains. However, this estimate is clearly low. The TolHe 2-color TOFMS contains both the peaks at 53 and 76 cm^{-1} above the

TolHe 0_0^0. The $TolHe_2$ species shows evidence of these features as well (see Fig. 6). These observations imply that the D_o for both species is greater than ~76 cm^{-1}.

The dominant features in the DE spectrum of TolHe 0^0 are similar to those in the Tol 0^0 DE spectrum. Under high resolution ($\Delta\nu$ ~ 5 cm^{-1}) a short progression in the ground state vdW stretching mode is evident. This feature is presented in Fig. 7. The observation of this short ground state progression emphasized both the similarity of the ground and excited state stretching vibrations and the strong $\Delta V = 0$ propensity rule for the vdW motion.

Emission arising from the excitation of higher vibronic levels of TolHe is much more complicated than that obtained by pumping the comparable Tol feature. The DE spectrum arising from the TolHe $6a^1$ level is quite congested (see Table III): some of the peaks in this emission can be identified as emission from a number of Tol excited vibronic levels. The relatively small binding energy of TolHe allows vibrational predissociation (VP) to a large number of lower levels of Tol. The intensity of any one distinct feature of the TolHe DE is much less than that of the comparable Tol feature because the total emission intensity is spread out over so many transitions. The emission found by pumping TolHe $6b^1$ is very similar to that found for $6a^1$. These data are summarized in Table IV. The presence of Tol $6a^1$ emission in this latter spectrum suggests that 73 cm^{-1}, the difference in energy between the $6b^1$ and $6a^1$ levels, may be enough energy to cause VP of the TolHe vdW complex. This would set an upper limit to the D_o for TolHe of roughly 73 cm^{-1}. This value and the apparent contradiction with the lower limit found above, will be discussed further in the next section.

Tol-CH_4

The Tol-CH_4 spectra appear to the low energy side of the comparable Tol vibronic features. The $TolCH_4$ 0_0^0 is shift -43 cm^{-1} from the Tol 0_0^0 and several vdW mode features can be identified between the $TolCH_4$ and Tol 0_0^0 transitions (see Fig. 8). Tentative assignments can be made for the vdW features and they are presented in Table V. $Tol(CH_4)_2$ exhibits an additive spectral shift for the 0_0^0 feature and a slightly more complicated set of v peaks. A vdW stretching progression similar to the one characterized for $TolCH_4$ is evident in addition to comparable bending modes. A relatively intense feature at $Tol(CH_4)_2$ 0_0^0 + 63 cm^{-1} can be tentatively assigned as either the independent stretching of both $TolCH_4$ bonds (a harmonic "double" excitation) or a second $Tol(CH_4)_2$ 0_0^0 for another configuration.

Larger clusters also absorb in this region as shown in Fig. 9. If the region between the $Tol(CH_4)_2$ 0_0^0 and 50 cm^{-1} to the low energy side of this feature is pumped, $Tol(CH_4)_x$ ($3 < x < 15$) clusters and $Tol_n(CH_4)_x$ $n = 2,3,4,\ldots$ and $x = 1,2,3,\ldots$) clusters are observed. Preliminary absorption spectra of some of these species reveal complicated structures; these spectra will be the subject of a future publication.

Higher vibronic transitions of $Tol(CH_4)_x$ evidence spectra that are quite similar to those just described for the 0_0^0 region. FE spectra of the $6a_0^1$ and $6b_0^1$ regions show patterns of $TolCH_4$ and Tol peaks that are nearly identical in appearance to the spectra of Fig. 8. The $TolCH_4$ vibronic

bands are red shifted 43 cm^{-1} from their respective Tol counterparts and vdW vibrational features are evident to the high energy side of the $TolCH_4$ vibronic origins. The Tol-CH_4 species also generate 2-color TOFMS in the $6a_0^1$ and $6b_0^1$ regions. This indicates that the $6b^1$ vibrational energy (533 cm^{-1}) is insufficient to cause vibrational predissociation of the $TolCH_4$ vdW cluster on the time scale of the experiment.[8] Since the $TolCH_4$ 1_0^1 transition is not observed with 2-color TOFMS detection, the dissociation energy for the vdW cluster can be bracketed between 533 and 739 cm^{-1}. Of course, FE spectra for Tol-CH_4 can be observed to much higher vibronic energies.

The $TolCH_4$ DE spectra are weak and much more congested than comparable Tol spectra. The $TolCH_4$ 0^0 DE spectrum evidences some weak features similar to those found in the Tol 0_0^0 DE spectrum; however, a large background of unassignable features is also present. A parallel set of spectra obtain for the $TolCH_4$ $6a^1$ DE. The $TolCH_4$ 1^1 DE spectra consists only of Tol 0_0^0 emission peaks, demonstrating that at this energy (733 cm^{-1}) the $TolCH_4$ undergoes vibrational predissociation on the time scale of the fluorescence lifetime (~70 ns). Even at this energy, however, a broad background of unassignable intensity is evident; the low intensity and broad background seem generally to characterize the $Tol(CH_4)_x$ emission.

VI. DISCUSSION

In this section a more in depth treatment of cluster geometry, solvent spectral shift, binding energy, and the comparison between solution and cluster properties will be presented. First, however, a few general remarks on the spectra are in order.

While the signal to noise ratio for the FE and 2-color TOFMS Tol cluster experiments is quite reasonable and roughly comparable to those for aniline clusters, the DE spectra are generally quite congested and low in intensity. We attribute this to four causes: 1) the overall emission intensity from toluene and toluene clusters appears relatively low due to the long lifetime of the fluorescence (~70 ns); 2) concentration of the clusters in the beam is kept low to optimize the spectral resolution of small cluster features; 3) VP seems to occur to a large number of lower vibronic levels of toluene; and 4) some of the emission is associated with $(Tol)_x$ and $(Tol)_x(solvent)_y$ whose absorption overlaps that of the clusters. The latter point in not trivial because the beam conditions which apparently favor vdW clusters (P_o 200 psi, room temperature toluene and nozzle) also seem to produce a substantial concentration of $(Tol)_x$ complexes.

Because of the poor quality of the DE spectra, it has not been possible thus far to characterize the intramolecular vibrational relaxation (IVR) processes for Tol-He or Tol-CH_4 cluster. It is clear, however, that the IVR process is important for this system; at levels for which VP occur, a much cleaner, more intense DE spectrum obtains. The characteristic times for the various processes - VP, IVR, second photon absorption, fluorescence - appear to be of the same order as found for the aniline cluster systems.[8] Thus, VP

is slower than 5 ps, IVR times lie between VP and fluorescence times, and the time taken to absorb the ionizing photon is longer than the VP time but shorter than the IVR time.

The last general point to be made concerning the Tol and Tol cluster spectra is derived from the 2-color TOFMS. The ionization beam energy set by the Tol 0_0^0 is not optimum for any of the Tol vibronic bands nor any of the Tol-CH_4 cluster bands. For the Tol vibronic features the ionization energy must be increased by about 100 cm^{-1} over the value predicted based on the Tol 0_0^0 ionization energy in order to maximize the 2-color TOFMS signal. The results for Tol CH_4 clusters are similar but not as dramatic. Much larger reductions in the optimum ionization energy are found for other toluene based systems (i.e., $(Tol)_x$, Tol-C_2H_6, Tol-C_3H_8).[9] Comparable data obtains for the aniline clusters studied thus far.[2a,b] These ionization energy changes have important consequences for 2-color TOFMS signal intensities and are, of course, important for the reduction of ion fragmentation.

A. Geometry

The geometry of the Tol-He and Tol-CH_4 vdW clusters can be reasonably well established based on calculations for other aromatic systems,[4a] spectral shift data for both toluene and aniline[2] clusters, and by analogy with other systems for which rotational spectra have been obtained.[1,3] For the tetrazine-He and tetrazine-Ar[1] clusters the rare gas atoms have been definitively demonstrated to bind above and below the aromatic ring such as to preserve the symmetry axis perpendicular to the plane; calculations indicate a similar structure for more general ring systems.[4a] For binding symetrically in this manner, additive spectral shifts for the first two ligands are found.

Thus, as we have concluded previously for An-He and An-CH_4, the first two ligands in Tol-He and Tol-CH_4 clusters add symmetrically above and below the plane of the ring. Clusters involving three ligand (either He and CH_4) around aniline or toluene yield absorption spectra very different from those associated with the smaller clusters. In particular, the clusters with three solvent molecules exhibit non-additive spectral shifts and their spectra contain at least one component which is broad and featureless. This points to the addition of the third ligand to a site perhaps less localized and inequivalent to the sites occupied by the first two ligands. The general properties and geometries of $Tol(CH_4)_x$ ($x \geq 3$) clusters present a rather complicated set of problems, however, and will be the subject of future reports from this laboratory.

B. Solvent Spectral Shift

While cluster geometry is typically controlled by repulsive interactions (proportional to $1/r^{12}$), interactions which generate the binding are associated with the dispersion or polarizability interaction (proportional to $1/r^6$)[4a]. Changes in these latter interactions upon excitation gives rise to solvent spectral shifts. The observed shifts should therefore scale with the solvent polarizability and changes in the solute polarizability upon excitation. Thus, aniline-methane and toluene-methane clusters have similar binding energies (nearly the same polarizabilities) but the aniline-methane clusters have a factor of two larger solvent shift. As we will report in future papers,[9] however, the (red) shift magnitude is not simply a function of solvent polarizability; it depends essentially on cluster geometry, solute/solvent interaction details, and on the proximity of other solvent molecules.

Helium seems to be an anomalous solvent system. in general; its polarizability is so small that other interactions, perhaps exchange, dominate the energetics of He-solute vdW complexes. Solvent shifts for the Tol-He system are slightly positive (1-3 cm^{-1}) and additive for the first two He atoms. No correlation is obvious between the properties of aniline and toluene and either the size or direction of the He solvent spectral shift; the aniline He shift is slightly negative (1-3 cm^{-1}) with respect to aniline monomer peaks for the first two atoms.[2] Whatever the nature of the He-solute interactions, it changes little upon solute excitation.

The solvent spectral shifts for larger clusters, Tol $(solvent)_x$ $x > 3$, are not additive and are in general quite dependent on the geometry of the particular cluster involved.[9] For these larger clusters certain geometries, at present not well characterized, possess shifts that converge around -150 cm^{-1}. This latter shift is quite comparable to the gas to liquid shift (177 cm^{-1}) reported for a toluene-methane solution[5a]; in fact, the two values are certainly identical within experimental resolution.

C. Binding Energy

The binding energy for Tol-He can be found in two different experiments; 2-color TOFMS and DE from high vibronic levels. The 2-color TOFMS for the 76 cm^{-1} methyl motion in the excited state sets a lower limit to the binding energy; that is, $D_o > 76$ cm^{-1}. Although the DE spectra from TolHe $6a^1$ and $6b^1$ are quite weak and the important regions are highly congested, the prominent features in the spectra can be assigned (see Tables III and IV). Several emission features in the TolHe $6a^1$ DE spectrum are

identified as originating from Tol 15^1: a firm upper limit of 91 cm^{-1}, based on the $6a^1$-15^1 energy gap, can thus be set for the binding energy. In addition, the weak congested emission from TolHe $6b^1$ appears to contain features originating from Tol $6a^1$. Although the assignments are less certain in this instance, the observations of Tol $6a^1$ emission would suggest an upper limit of 73 cm^{-1} (the $6b^1$-$6a^1$ energy separation) to the binding energy. While this upper limit seems in conflict with the 2-color TOFMS derived lower limits of 76 cm^{-1}, a number of kinetic processes could be invoked to rationalize the apparent difficulty. A value of the Tol-He $D_o \sim 75$ cm^{-1} is not unreasonable but it is probably best to suggest that $75 \leq D_o \leq 90$ cm^{-1}.

Note that this binding energy is approximately one-half of that found for aniline-He. However, the polarizabilities of aniline and toluene are both 11 ± 10% $Å^3$ in the ground state[10]; the ground and excited state binding energy are expected to be nearly identical based on the small spectral shifts.

The binding energy for Tol-CH_4 is indistinguishable from that of aniline-CH_4; D_o lies between 533 and 739 cm^{-1}. The correlation between polarizability and binding energy should not be extrapolated to other systems, however; it does not hold. for example, for toluene solvated by ethane and propane for which detailed structure and geometry can produce nearly a factor of two change in the binding energy.[9]

D. Solution Properties

Parallels between solution properties and cluster spectral shifts, binding energies, and dynamics (VP and IVR) have already been mentioned in our previous publications.[2a,b] The new information derived from the Tol-CH_4 system concerns the trends in the absorption spectra as larger clusters are

probed. From $TolCH_4$ and $Tol(CH_4)_2$ spectra it is clear that the $Tol-CH_4$ liquid shift of -177 cm^{-1} [5a] is rapidly approached by the clusters. This trend seems to be continued by at least a component of the $Tol(CH_4)_3$ spectrum. Furthermore, the ubiquitous presence of intensity in the $Tol(CH_4)_3$ mass channel as the laser is tuned throughout this region attests to the diffuse nature of this absorption. Such a diffuse absorption is also a characteristic of the solution spectrum. From these observations it seems clear that at least one geometry of the $Tol(CH_4)_2$ species is approaching solution-like properties.

V. CONCLUSIONS

The following table summarizes the data (in cm^{-1}) for the toluene-helium and toluene-methane clusters:

Species	Solvent Shift	Stretching Frequency		Binding Energies
		V_1	V^1	
TolHe	1.5	11	9.0	75-90
$TolHe_2$	3.0		8.8	
$TolCH_4$	-43		31.8	533-739
$Tol(CH_4)_2$	-83		32.5	

For the Tol-He and Tol-CH_4 clusters the first two ligands add above and below the plane of the aromatic ring. The third ligand is suggested to bind in the plane of the ring, probably near the CH_3 group. Three coordinated CH_4 solvent molecules appear to generate spectral shifts and linewidths similar to those found for toluene-methane solutions. $TolHe_3$ also generates a broad spectrum, shifted only slightly from $TolHe_2$; higher mass clusters fall within the $TolHe_3$ spectrum.

Studies of toluene and aniline solvated by ethane and propane are now in progress; the results will be reported in the near future. Based on these studies, however, caution should be exercised in drawing general conclusions concerning the nature and strength of the interactions, binding energies, and solvent spectral shifts if information on detailed cluster structure is not available. Calculations are also in progress which should generate an assessment of cluster structure and its effect on binding energy, solvent shift, and transition linewidth.

REFERENCES

1 a. R.E. Smalley, L. Wharton, D.H. Levy and D.W. Chandler, J. Chem. Phys. 68, 2487 (1978).

b. D.V. Brumbaugh, J.E. Kenny and D.H. Levy, J. Chem. Phys. 78, 3415 (1983).

2 a. E.R. Bernstein, K. Law and Mark Schauer, J. Chem. Phys. 80, XXXX (1984).

b. E.R. Bernstein, K. Law and Mark Schauer, J. Chem. Phys. 80, XXXX (1984).

c. A. Amirav, U. Even, J. Jortner and B. Dick, Mol. Phys. 49, 899 (1983).

3 a. S.M. Beck, M.G. Liverman, D.L. Monts and R.E. Smalley, J. Chem. Phys. 70, 232 (1979).

b. K.H. Fung, W.E. Henke, T.R. Hays, H.L. Selzle and E.W. Schlag, J. Phys. Chem. 85, 3560 (1981).

4 a. M.J. Ondrechen, Z. Berkovitch-Yellin and J. Jortner, J. Am. Chem. Soc. 103, 6586 (1981).

b. A. Amirav, U. Even and J. Jortner, J. Chem. Phys. 75, 2489 (1981).

c. A.W. Castleman, Jr., B.D. Kay, V. Hermann, P.M. Holland and T.D. Mark, Surf. Sci. 106, 179 (1981).

d. K.L. Saenger, G.M. McClelland and D.R. Herschbach, J. Phys. Chem. 85, 3333 (1981).

e. T.R. Hays, W. Henke, H.L. Selzle and E.W. Schlag, Chem. Phys. Lett. 77, 19 (1981).

f. P.M. Felker and A.H. Zewail, Chem. Phys. Lett. 94, 454 (1983).

5 a. J. Lee, F. Li and E.R. Bernstein, J. Phys. Chem. 87, 1180 (1983).

b. J. Lee, F. Li and E.R. Bernstein, J. Phys. Chem. 87, 1175 (1983).

c. F. Li, J. Lee and E.R. Bernstein, J. Phys. Chem. 87, 254 (1983).

d. J. Lee, F. Li and E.R. Bernstein, J. Phys. Chem. 87, 260 (1983).

e. F. Li, J. Lee and E.R. Bernstein, J. Phys. Chem. 86, 3606 (1982).

f. M.W. Schauer, J. Lee and E.R. Bernstein, J. Chem. Phys. 76, 2773 (1982).

g. E.R. Bernstein and J. Lee, J. Chem. Phys. 74, 3159 (1981).

6 a. J. Murakami, M. Ito and K. Kaya, Chem. Phys. Lett 80, 203 (1981).

b. J.B. Hopkins, D.E. Powers and R.E. Smalley, J. Chem. Phys. 72, 5039 (1980).

c. J.B. Hopkins, D.E. Powers, S. Mukamel and R.E. Smalley, J. Chem. Phys. 72, 5049 (1980).

7. G. Varsanyi, "Assignments for Vibrational Spectra of Seven Hundred Benzene Derivatives" (Wiley and Sons, New York, 1974).

8. For further discussion of the time scale of various energy dissipation pathways, see ref. 2b.

9. E.R. Bernstein, K. Law and Mark Schauer, unpublished results.

10 a. A.K. Burnham and T.D. Gierke, J. Chem. Phys. 73, 4822 (1980).

b. R.J.W. LeFevre and L. Radom, J. Chem. Soc. 1967, B 1295.

c. M. Aroney and R.J.W. LeFevre, J. Chem. Soc. 1960, 2161.

TABLE I

The toluene FE spectrum in the region encompassing Tol 0_0^0 and Tol $6a_0^1$ (see Fig. 1).

WAVELENGTH (vac Å)	ENERGY (vac cm^{-1})	RELATIVE ENERGY (cm^{-1})	ASSIGNMENT
2669.67	37457.7	-19.7	Tol_2 0_0^0
2668.26	37477.5	0	0_0^0
2664.48	37530.8	53.3	T_0^x
2662.83	37554.0	76.5	T_0^y
2647.90	37765.7	288.2	$10b_0^2$
2647.71	37768.5	291.0	$16a_0^2$
2645.01	37807.0	329.5	15_0^1
2642.31	37845.6	368.1	$16b_0^1$
2636.34	37931.4	453.9	Tol_2 $6a_0^1$
2635.97	37936.7	459.2	$6a_0^1$
2635.73	37940.1	462.6	$6a_0^1$
2635.04	37950.1	472.6	?

TABLE II

TolHe and $TolHe_2$ 2-color TOFMS in the 0_0^0 region (see Fig. 6).

ENERGY (vac cm^{-1})	RELATIVE ENERGY (cm^{-1})	ASSIGNMENT[a]
TolHe (1.55 cm^{-1} relative to Tol 0_0^0)		
37479.1	0	TolHe 0_0^0
37488.2	9.1	TolHe V_0^1
37494.6	15.5	TolHe V_0^2
$TolHe_2$ (3.18 cm^{-1} relative to Tol 0_0^0)		
37480.7	0	$TolHe_2$ 0_0^0
37489.5	8.85	$TolHe_2$ V_0^1
37495.4	14.7	$TolHe_2$ V_0^2

a) V refers to the vdW stretching mode.

TABLE III

DE spectrum obtained as TolHe $6a_0^1$ is pumped. Only the prominent peaks in the spectrum are reported.

WAVELENGTH (vac Å)	ENERGY (vac cm^{-1})	ENERGY RELATIVE TO TOL 0_0^0 (cm^{-1})	CALCULATED RELATIVE ENERGY (cm^{-1})	ASSIGNMENT[a]
2668.4	37475	2	0	0_0^0
2668.7	37470	7	14	15_1^1
2672.7	37415	62	62	$6a_1^1$
2674.6	37388	89	96	$16b_1^1$
2675.6	37375	103	104	$15_0^1 10b_2^0$
2677.4	37350	127	120	$10b_0^2 16a_1^0$
2678.7	37331	146	146	$10b_2^2$
2679.3	37324	154	153	$16b_0^1 6a_1^0$
2680.7	37303	175	173	$16a_0^2 16b_1^0$
2681.2	37297	181	176	$10b_0^2 16b_1^0$
2683.4	37266	211		$6a_0^1 X_1^0$
2685.1	37243	234	233	$10b_0^2 6a_1^0$

a) All fluorescence seems to originate from Tol monomer. X denotes an unknown level in the ground state.

TABLE IV

DE spectrum obtained as TolHe $6b_0^1$ is pumped. Only the prominent peaks in the spectrum are reported.

WAVELENGTH (vac Å)	ENERGY (vac cm^{-1})	ENERGY RELATIVE TO TOL 0_0^0 (cm^{-1})	CALCULATED RELATIVE ENERGY (cm^{-1})	ASSIGNMENT[a]
2668.3	37477	0	0	0_0^0
2669.4	37462	16	14	15_1^1
2673.2	37409	69	62	$6a_1^1(16b_0^1 10b_2^0)$
2674.3	37393	84	78	$15_0^1 16a_1^0$
2675.6	37375	103	104	$15_0^1 10b_2^0$
2679.1	37326	151	146	$10b_2^2$
2679.5	37321	156	153	$16b_0^1 6a_1^0$
2681.1	37298	179	176	$10b_0^2 16b_1^0$
2683.2	37269	209		$6a_0^1 X_1^0$
2685.3	37240	237	233	$10b_0^2 6a_1^0$

a) All fluorescence seems to originate from the Tol monomer. X denotes an unknown level in the ground state.

TABLE V

Two color TOFMS of $TolCH_4$ and $Tol(CH_4)_2$ in the 0_0^0 region. Only the prominent peaks are tabulated and tentative assignments are given (see Fig. 8).

ENERGY (vac cm^{-1})	RELATIVE ENERGY (cm^{-1})	ASSIGNMENT[a]
$TolCH_4$ (-43 cm^{-1} relative to Tol 0_0^0)		
37434.4	0	$TolCH_4$ 0_0^0
37451.8	17	$TolCH_4$ A_0^1
37458.7	24	$TolCH_4$ B_0^1
37466.2	32	$TolCH_4$ V_0^1
37488.5	54	$TolCH_4$ V_0^2
$Tol(CH_4)_2$ (-83 cm^{-1} relative to Tol 0_0^0)		
37394.1	0	$Tol(CH_4)_2$ 0_0^0
37412.6	18	$Tol(CH_4)_2$ A_0^1
37418.5	24	$Tol(CH_4)_2$ B_0^1
37426.7	32	$Tol(CH_4)_2$ V_0^1
37440.5	46	$Tol(CH_4)_2$ $V_0^1A_0^1$
37446.2	52	$Tol(CH_4)_2$ V_0^2
37456.9	63	$Tol(CH_4)_2$

a) Tentative assignments are as follows: V stands for the Tol-CH_4 stretch, and A and B are different vdW bonds. The feature at $Tol(CH_4)_2$ 0_0^0 + 63 cm^{-1} can be assigned as either a simultaneous double excitation of independent stretches of both Tol-CH_4 bonds or the 0_0^0 of a new configuration of $Tol(CH_4)_2$.

FIGURE CAPTIONS

FIGURE 1

Portions of the FE spectrum of toluene in the region encompassing Tol 0_0^0 and Tol $6a_0^1$. For this spectrum P_o = 150 psi. Some of the peaks are due to Tol_2 species. No $TolHe_x$ peaks are present (see Table I).

FIGURE 2

FE spectrum of toluene expanded in He at high (upper trace) and low backing pressures. The energy scale is relative to Tol 0_0^0 (37477.5 cm^{-1}). Note the vdW cluster peaks to the blue of the Tol 0_0^0.

FIGURE 3

FE spectra for the $6b_0^1$ region at high (upper trace) and low backing pressures of He. The energy scale is relative to Tol $6b_0^1$ (38010.5 cm^{-1}). Note the similarity in the pattern of vdW peaks with that found in the 0_0^0 region. Some intensity due to Tol_2 species is evident to the red of Tol $6b_0^1$.

FIGURE 4

FE spectra for the $6a_0^1$ region at high (upper trace) and low backing pressures of He. Due to Fermi resonance, the Tol $6a_0^1$ is a doublet. Consequently vdW peaks of the lower energy feature interfere with those of the higher energy feature. Also, intensity due to Tol_2 is evident to the low energy side of the Tol $6a_0^1$ transition. The energy scale is relative to the lower energy Tol $6a_0^1$ feature (37937.5 cm^{-1}).

FIGURE 5

Two-color TOFMS of Tol and several $TolHe_x$ clusters in the 0_0^0 region. Some fragmentation is evident in the Tol spectra as shown by the presence of some intensity due to Tol_2 and $TolHe_x$ features. However in the $TolHe_x$ 2-color TOFMS spectra the pump beam intensity was kept below ~100 μj/pulse and fragmentation is not evident.

FIGURE 6

Expanded 2-color TOFMS of Tol and $TolHe_x$ in the 0_0^0 region. The 0_0^0 peaks have been artificially aligned at 0 relative energy. Note the similarity in the vdW stretch progression for TolHe and $TolHe_2$. Also, note the presence of TolHe T_o^x and T_o^y peaks (see Table II).

FIGURE 7

Part of the high resolution DE spectrum of Tol 0^0 and TolHe 0^0. The feature at -18 cm^{-1} relative to the main peak in both spectra is due to Tol_2. The energy scale is relative to Tol $6b_1^0$. Note the V_1^0 peak which gives the energy of a vdW mode in the ground state.

FIGURE 8

Two-color TOFMS of $TolCH_4$ (upper trace) and $Tol(CH_4)_2$ in the 0_0^0 region. The energy scale is relative to Tol 0_0^0 (37477.5 cm^{-1}). Note the peaks due to vdW stretches and bends. Tentative assignments are given in Table V.

FIGURE 9

One-color TOFMS of $Tol(CH_4)_x$ clusters which absorb in the region of the $Tol(CH_4)_2$ 0_0^0. The upper trace identifies the species which absorb at the $Tol(CH_4)_2$ 0_0^0 position (37394.5 cm^{-1}). The intensity in the Tol and $TolCH_4$ mass channels is due to fragmentation of larger ions. The lower trace identifies the species which absorb to the red of $Tol(CH_4)_2$ (37370 cm^{-1}); the intensity in the Tol, $TolCH_4$ and $Tol(CH_4)_2$ mass channels is due to fragmentation of larger ions. Note the presence of $Tol_2(CH_4)_y$ clusters and very large $Tol_x(CH_4)_y$ clusters.

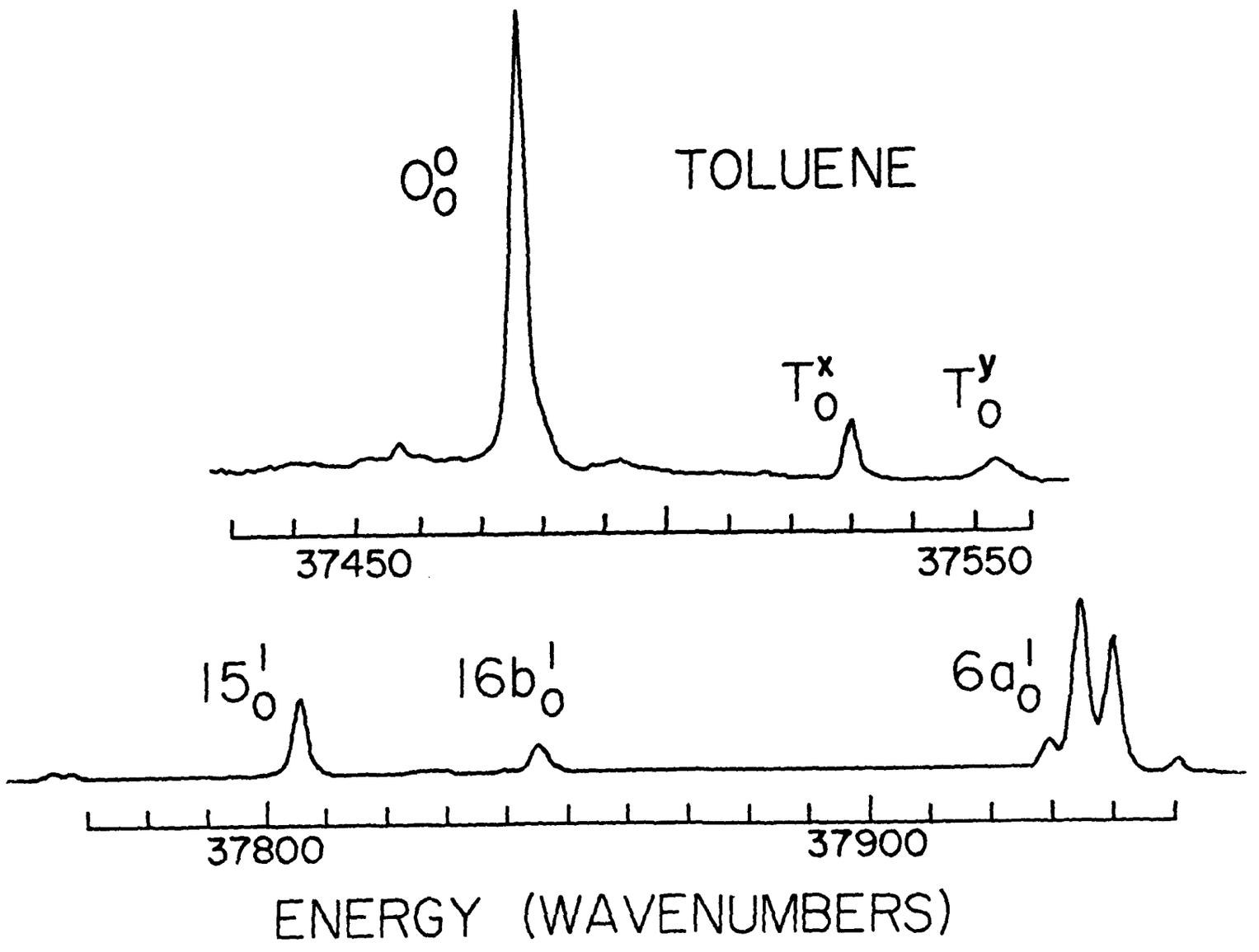
0_0^0
TOLUENE
T_0^x
T_0^y
37450
37550
15_0^1
$16b_0^1$
$6a_0^1$
37800
37900
ENERGY (WAVENUMBERS)

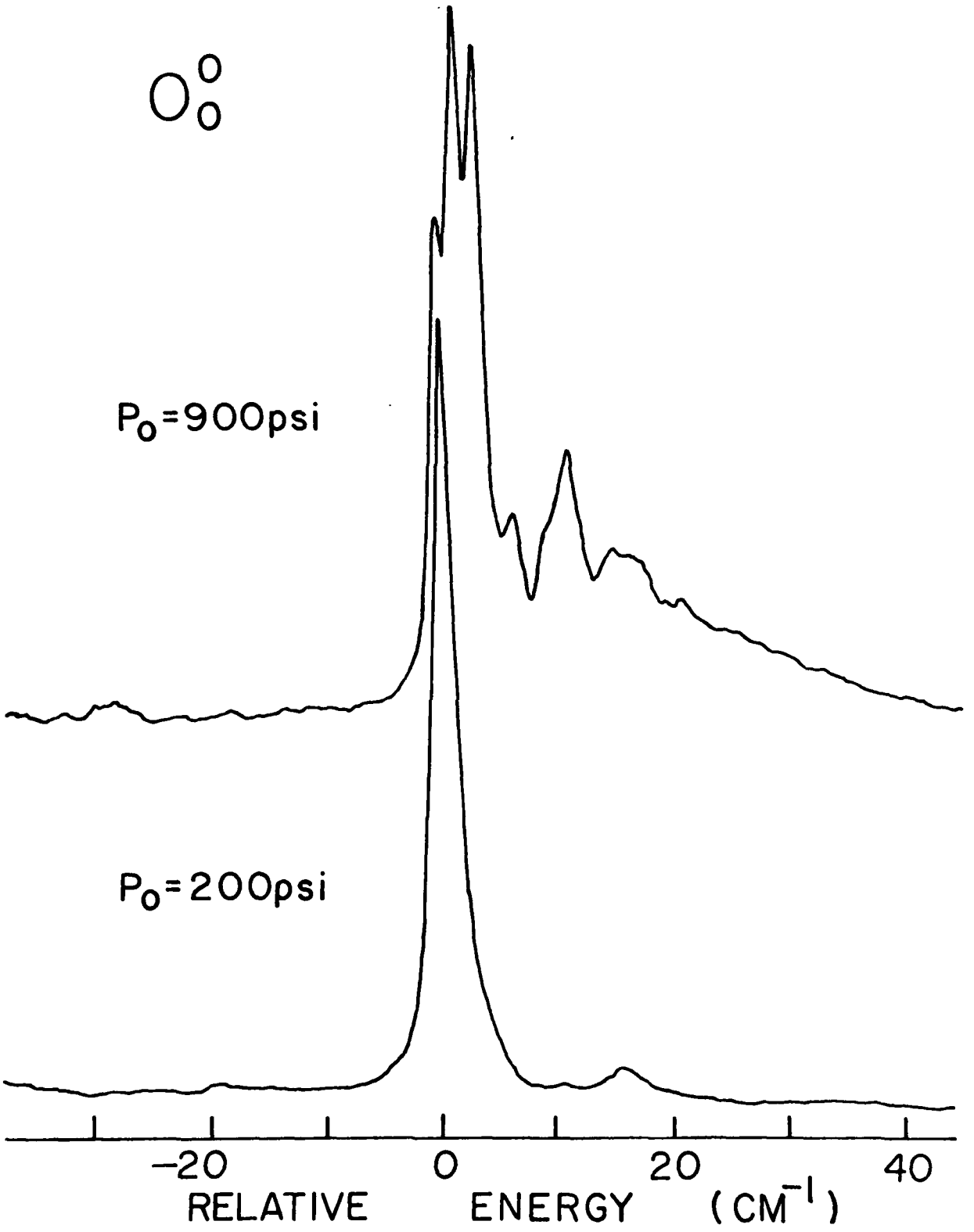
O_0^0
P_0=900psi
P_0=200psi
−20
0
20
40
RELATIVE ENERGY (CM^{-1})

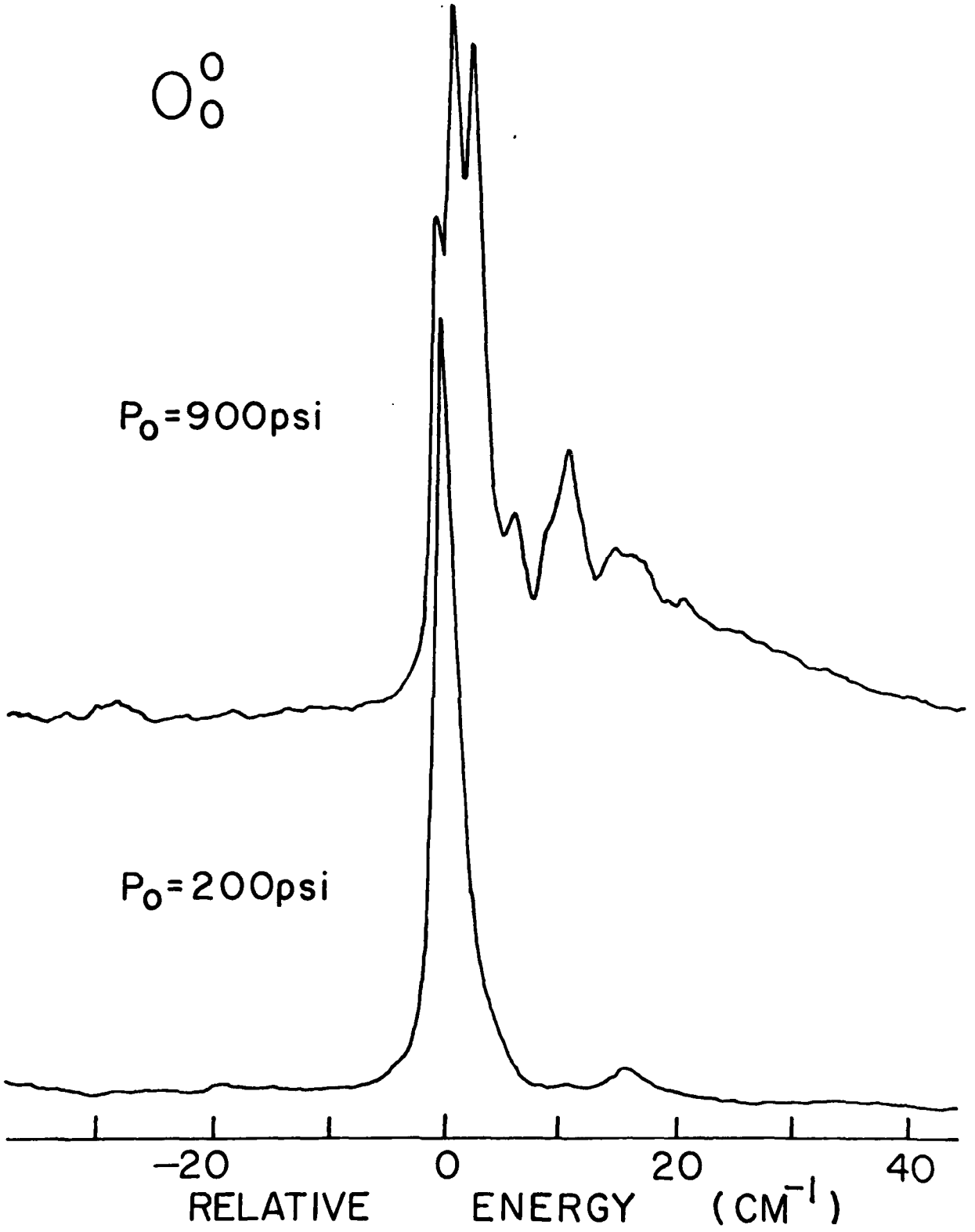
O_0^0
P_0=900psi
P_0=200psi
−20
0
20
40
RELATIVE ENERGY (CM^{-1})

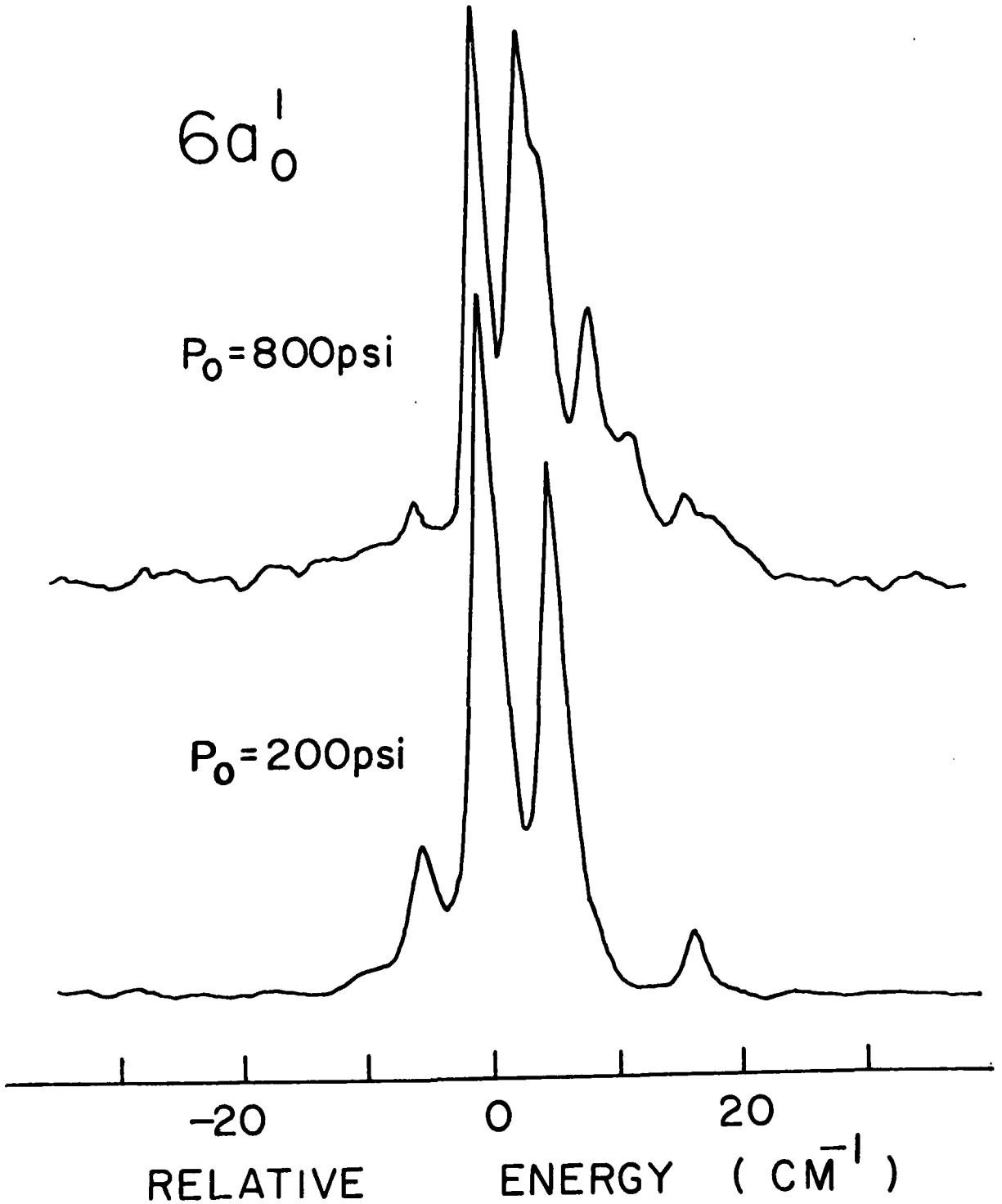
$6a_0^1$
P_0=800psi
P_0=200psi
-20
0
20
RELATIVE ENERGY (CM^{-1})

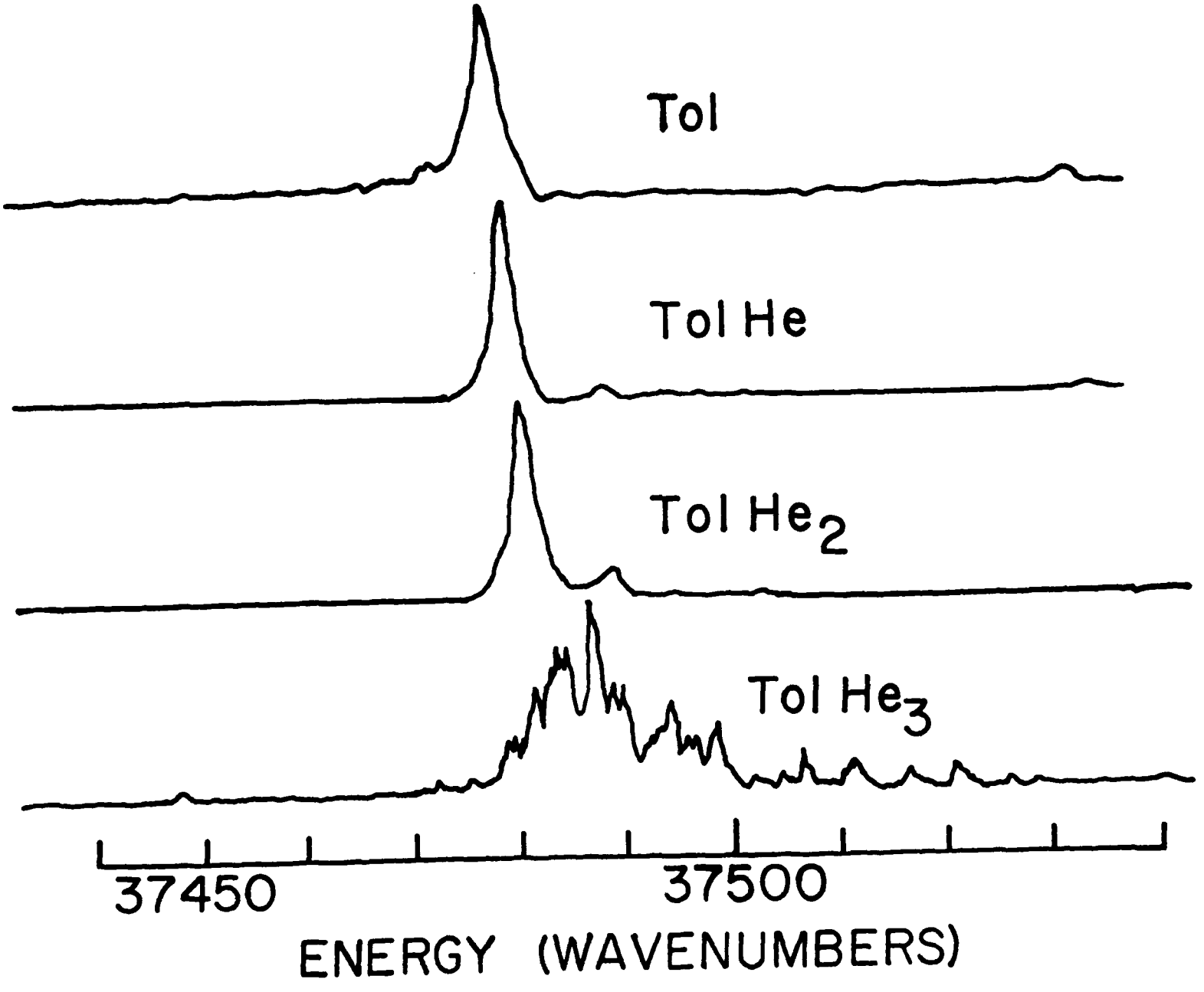
Tol
Tol He
Tol He2
Tol He3
37450
37500
ENERGY (WAVENUMBERS)

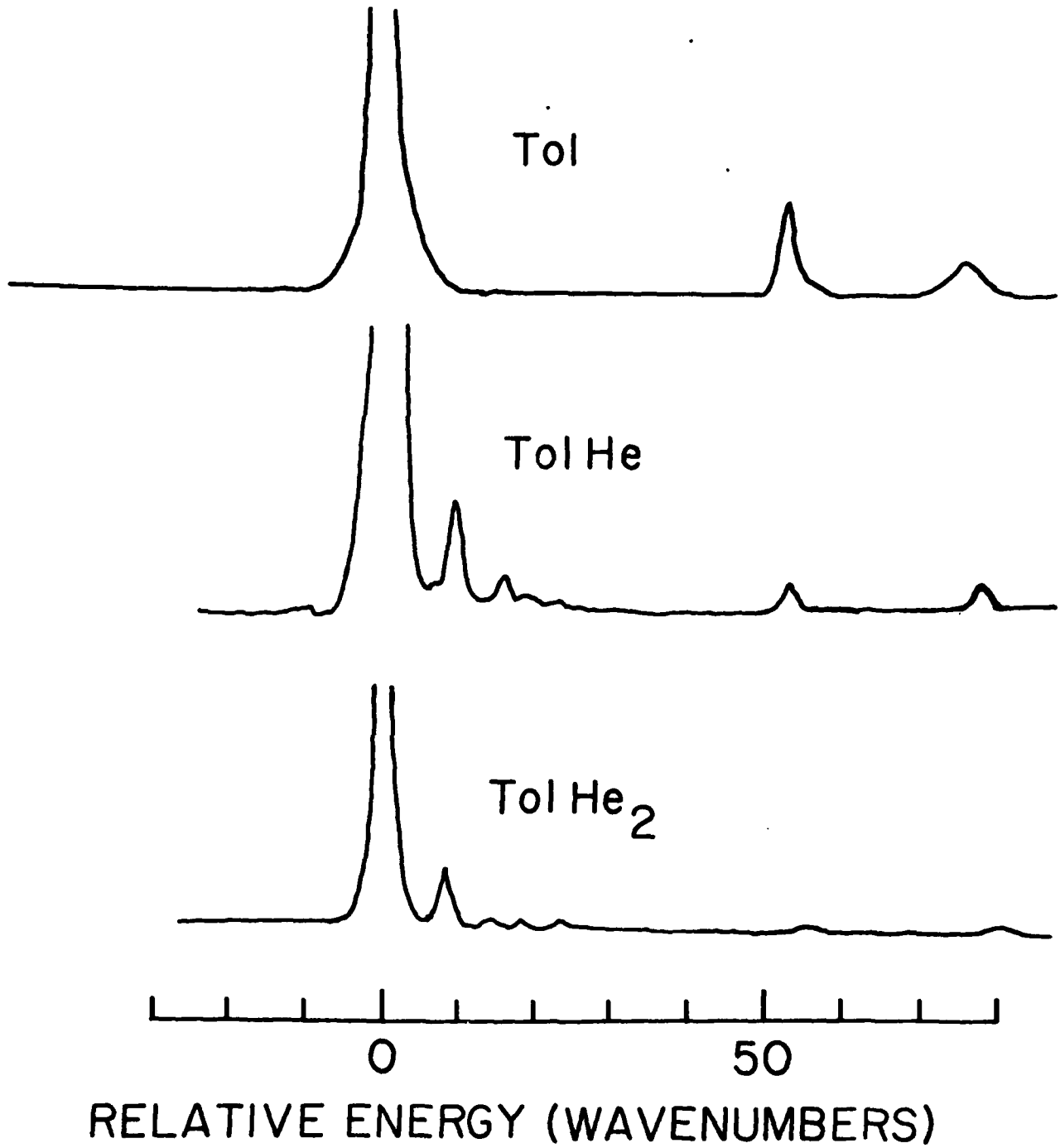
TolI
TolIHe
TolIHe2
0
50
RELATIVE ENERGY (WAVENUMBERS)

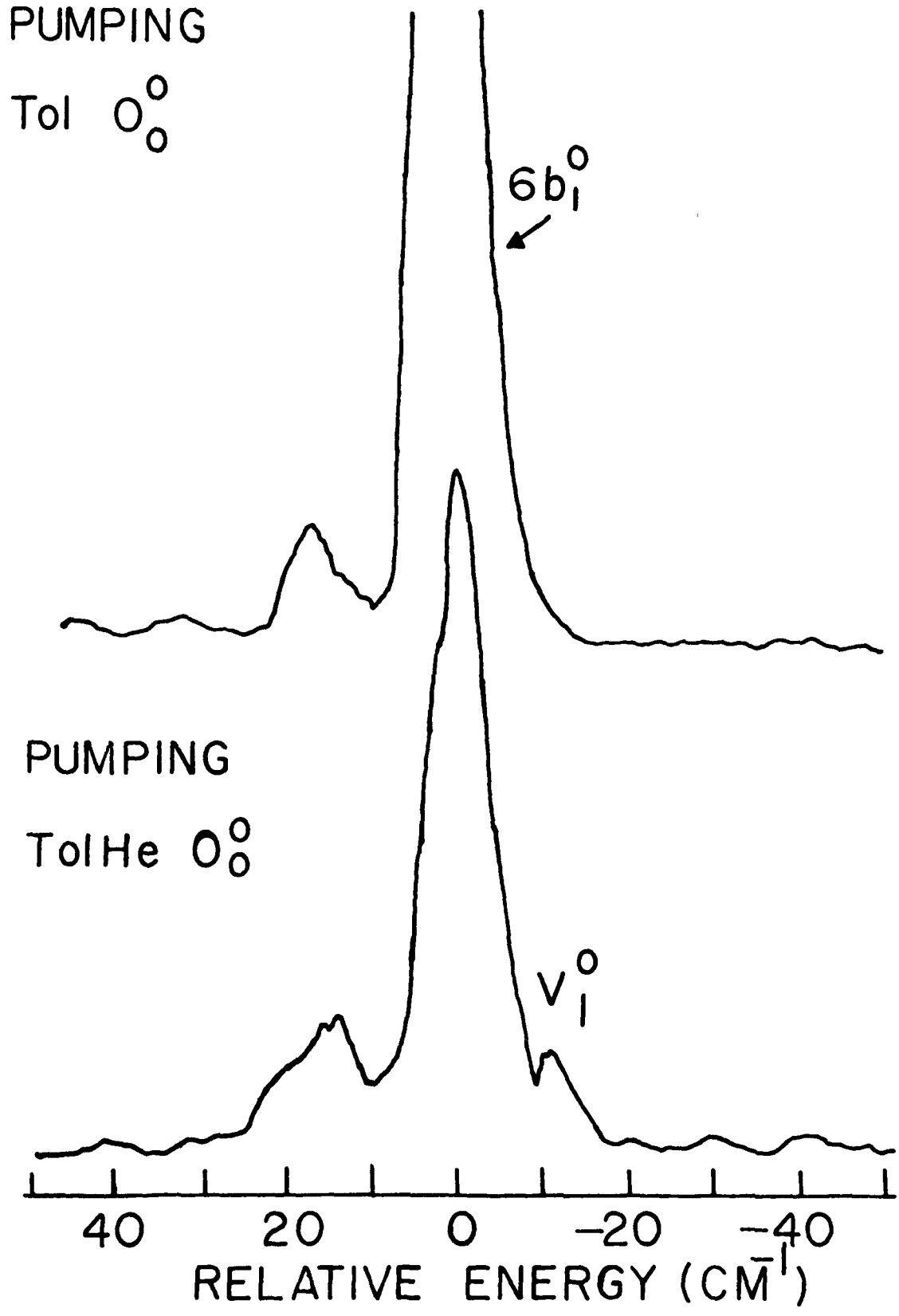
PUMPING
Tol 0_0^0
$6b_1^0$
PUMPING
TolHe 0_0^0
v_1^0
40
20
0
-20
-40
RELATIVE ENERGY (CM^{-1})

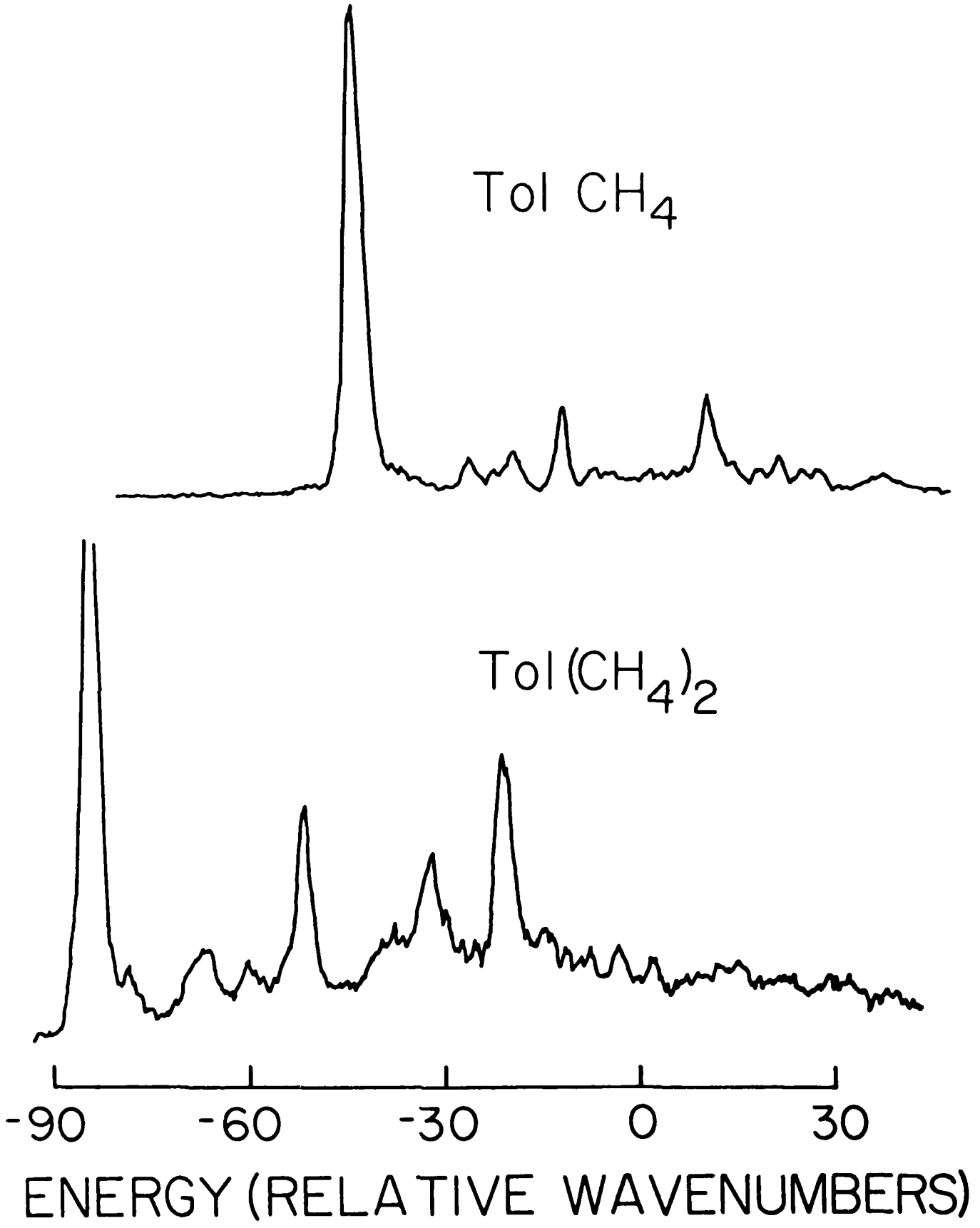
Tol CH_4
Tol $(CH_4)_2$
-90
-60
-30
0
30
ENERGY (RELATIVE WAVENUMBERS)

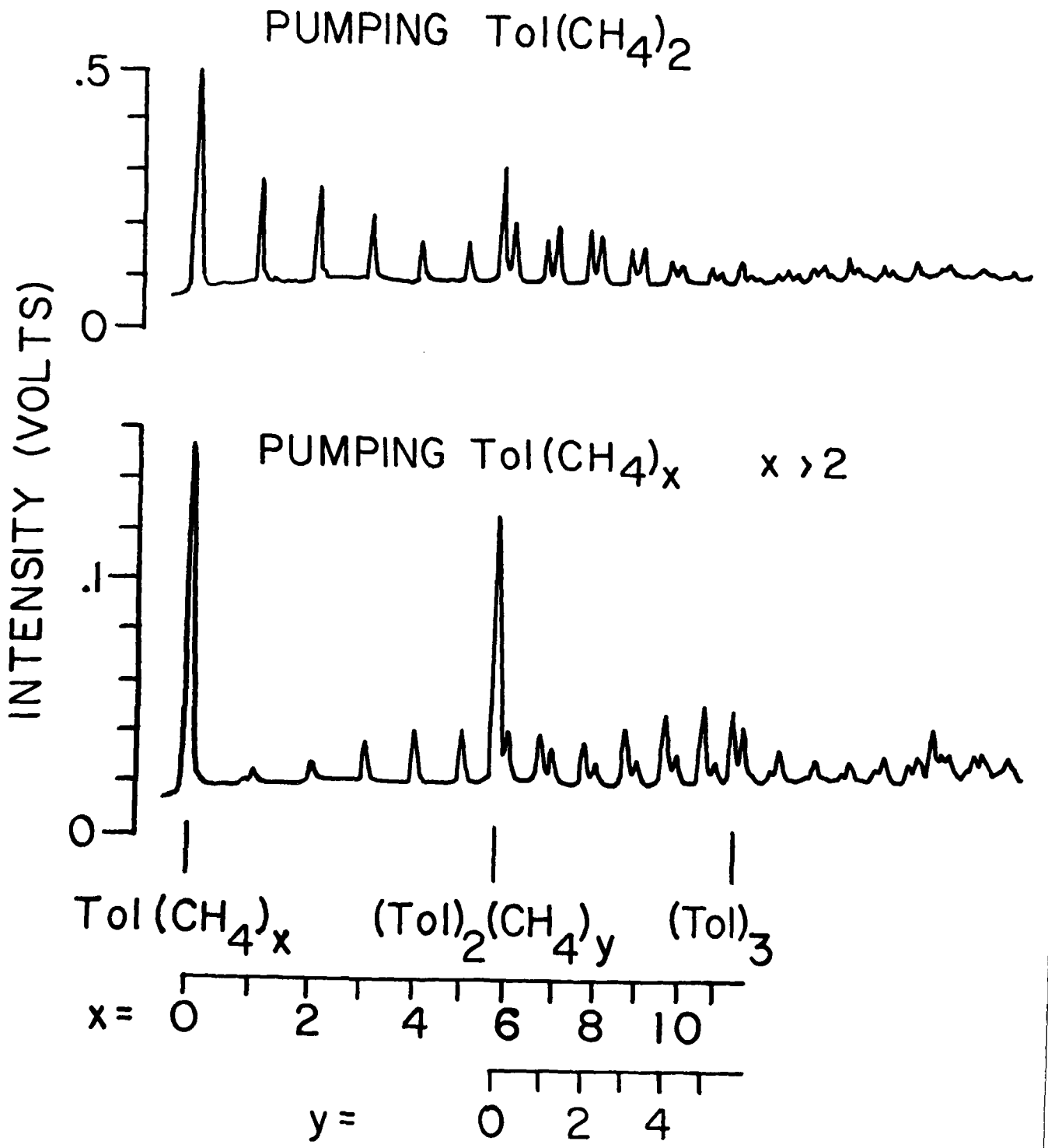
PUMPING Tol(CH4)2
.5
0
PUMPING Tol(CH4)x x > 2
INTENSITY (VOLTS)
.1
0
Tol(CH4)x
(Tol)2(CH4)y
(Tol)3
x= 0 2 4 6 8 10
y= 0 2 4

TECHNICAL REPORT DISTRIBUTION LIST, GEN

	No. Copies
Office of Naval Research Attn: Code 472 800 North Quincy Street Arlington, Virginia 22217	2
ONR Western Regional Office Attn: Dr. R. J. Marcus 1030 East Green Street Pasadena, California 91106	1
ONR Eastern Regional Office Attn: Dr. L. H. Peebles Building 114, Section D 666 Summer Street Boston, Massachusetts 02210	1
Director, Naval Research Laboratory Attn: Code 6100 Washington, D.C. 20390	1
The Assistant Secretary of the Navy (RE&S) Department of the Navy Room 4E736, Pentagon Washington, D.C. 20350	1
Commander, Naval Air Systems Command Attn: Code 310C (H. Rosenwasser) Department of the Navy Washington, D.C. 20360	1
Defense Technical Information Center Building 5, Cameron Station Alexandria, Virginia 22314	12
Dr. Fred Saalfeld Chemistry Division, Code 6100 Naval Research Laboratory Washington, D.C. 20375	1
U.S. Army Research Office Attn: CRD-AA-IP P.O. Box 1211 Research Triangle Park, N.C. 27709	1
Naval Ocean Systems Center Attn: Mr. Joe McCartney San Diego, California 92152	1
Naval Weapons Center Attn: Dr. A. B. Amster, Chemistry Division China Lake, California 93555	1
Naval Civil Engineering Laboratory Attn: Dr. R. W. Drisko Port Hueneme, California 93401	1
Department of Physics & Chemistry Naval Postgraduate School Monterey, California 93940	1
Scientific Advisor Commandant of the Marine Corps (Code RD-1) Washington, D.C. 20380	1
Naval Ship Research and Development Center Attn: Dr. G. Bosmajian, Applied Chemistry Division Annapolis, Maryland 21401	1
Naval Ocean Systems Center Attn: Dr. S. Yamamoto, Marine Sciences Division San Diego, California 91232	1
Mr. John Boyle Materials Branch Naval Ship Engineering Center Philadelphia, Pennsylvania 19112	1

SP482-3/A23

472:GAN:716:ddc
78u472-608

TECHNICAL REPORT DISTRIBUTION LIST, 051A

	No. Copies
Dr. M. A. El-Sayed Department of Chemistry University of California, Los Angeles Los Angeles, California 90024	1
Dr. C. A. Heller Naval Weapons Center Code 6059 China Lake, California 93555	1
Dr. J. R. MacDonald Chemistry Division Naval Research Laboratory Code 6110 Washington, D.C. 20375	1
Dr. G. B. Schuster Chemistry Department University of Illinois Urbana, Illinois 61801	1
Dr. A. Adamson Department of Chemistry University of Southern California Los Angeles, California 90007	1
Dr. M. S. Wrighton Department of Chemistry Massachusetts Institute of Technology Cambridge, Massachusetts 02139	1
Dr. M. Rauhut Chemical Research Division American Cyanamid Company Bound Brook, New Jersey 08805	1
Dr. J. I. Zink Department of Chemistry University of California, Los Angeles Los Angeles, California 90024	1
Dr. D. Haarer IBM San Jose Research Center 5600 Cottle Road San Jose, California 95143	1
Dr. John Cooper Code 6130 Naval Research Laboratory Washington, D.C. 20375	1
Dr. William M. Jackson Department of Chemistry Howard University Washington, DC 20059	1
Dr. George E. Walraffen Department of Chemistry Howard University Washington, DC 20059	1

TECHNICAL REPORT DISTRIBUTION LIST, GEN

	No. Copies
Mr. James Kelley DTNSRDC Code 2803 Annapolis, Maryland 21402	1
Mr. A. M. Anzalone Administrative Librarian PLASTEC/ARRADCOM Bldg 3401 Dover, New Jersey 07801	1